2020 IEEE International Conference on Robotics and Automation (ICRA)
31 May - 31 August, 2020. Paris, France

A Practical Climbing Robot for Steel Bridge Inspection

Son T. Nguyen, Anh Q. Pham, Cadence Motley, Hung M. La, *IEEE Senior Member*

***Abstract*— The advanced robotic and automation (ARA) lab has developed and successfully implemented a design inspired by many of the various cutting edge steel inspection robots to date. The combination of these robots concepts into a unified design came with its own set of challenges since the parameters for these features sometimes conflicted. An extensive amount of design and analysis work was performed by the ARA lab in order to find a carefully tuned balance between the implemented features on the ARA robot and general functionality. Having successfully managed to implement this conglomerate of features represents a breakthrough to the industry of steel inspection robots as the ARA lab robot is capable of traversing most complex geometries found on steel structures while still maintaining its ability to efficiently travel along these structures; a feat yet to be done until now.**

I. Introduction

According to the Federal Highway Administration [1], almost one third of 607,380 bridges in the United States are steel bridges. The National Bridge Inventory (NBI) [1] indicated that 25% of these steel bridges are either deficient or functionally obsolete, indicating a growing threat to the safety of transportation. A number of bridges collapsed recently (e.g., collapse of the I-5 Skagit River Bridge [2]) strongly suggests for more frequent inspection.

The growing number of bridge collapses has shown a significant impact on the safety of travelers. The current inspection practices for these bridges is mainly through visual and manual evaluations. These jobs tend to be very time consuming and dangerous, as a result there are not enough people willing and capable enough to do these jobs. This shortage in supply means that the demand for adequate inspection and maintenance of these bridges is not being met, [1], [3]. Therefore, there is a societal need for alternative solutions because the current methods are not able to satisfy the growing demand for safe, cost-effective, accurate inspection. One solution to meet this demand is through automated inspection with robots.

Civil infrastructures like bridges start their maintenance processes through inspectors who physically review the status of each steel member by tapping a hammer on the steel to collect impact echo waves for fatigue crack inspection [4], or visually looking at all of the surfaces of the steel members in order to detect for shallow surface cracks. The described procedure is very time consuming and not efficient. Often, it is dangerous for the inspectors to climb up and hang on cables to inspect the nearly inaccessible structures of bridges [5]. Additionally, some areas of these structures are very hard to reach or may not be accessible at all through conventional means. For example, the Golden Gate bridge, a landmark of the Bay area in San Francisco, California, is manually inspected by a team of 12 rope certified bridge engineers [5], who have to climb and hang on the high steel structures to perform inspection. As an effort to automate the inspection process, there has been a variety of climbing robot developments in recent years.

There are several designs based on conventional mobile robots. Some make use of tank-like tracks to enhance the friction of the robot on the steel surfaces they adhere to [6], [7]. Others function as magnetic wheeled robots [8]–[10] or roller chain-liked robot [11]. Notable developments of climbing robots for steel bridge/structure inspection can be seen in [12]–[22]. The adhesion force for tank-like types of inspection robots is typically created by magnets attached on the robot's roller chains [11], on the robot's wheels/sprockets, or on the robot body (untouched magnets). These magnets are kept in close proximity with the steel surfaces that these robots adhere to. Each of the measures has particular merits in differently working condition. Touched magnets on a roller chain or wheels allow the robot to transfer seamlessly between surfaces at 90 degree angles as well as other sharp angles, which might appear on a bridge [7], [23]–[29]. Tank-like robots with untouched permanent magnets help to allow the robots to pass small struggles like nuts and prevent loss of adhesion force when crossing rusty areas of steel [30]. Some improved wheel robots with soft frames make them more adaptive on a wider range of surfaces [31].

Imitation of mobility of climbing creatures is another approach. A spider-like robot with electromagnets on its feet was reported [32], and a legged robot was developed [33]. An inchworm-like robot [18] was an efficient design and creation, for Sydney bridge, Australia. This robot excels in its ability to transfer smoothly 360^o to other surfaces surfaces. It is equipped with a camera and sensors for structure 3D mapping.

Aerial robots provide great means for visual inspection tasks, especially with the cutting edge image processing technology of the present date. A variety of research in this area has been conducted. Some of the latest developments make drone control significantly safer in confined spaces

This work is supported by the U.S. National Science Foundation (NSF) under grants NSF-CAREER: 1846513 and NSF-PFI-TT: 1919127, and the U.S. Department of Transportation, Office of the Assistant Secretary for Research and Technology (USDOT/OST-R) under Grant No. 69A3551747126 through INSPIRE University Transportation Center.The views, opinions, findings and conclusions reflected in this publication are solely those of the authors and do not represent the official policy or position of the NSF and USDOT/OST-R.

The authors are with the Advanced Robotics and Automation (ARA) Lab, Department of Computer Science and Engineering, University of Nevada, Reno, NV 89557, USA. Anh Pham, from Duy Tan University, conducted this research when he was a visiting scholar at ARA Lab. Corresponding author: Hung La, email: hla@unr.edu.

[34], [35]. One innovation created a Quadcopter design with a clip to hold onto a bridge's beams to be stationary for inspection without wasting flying energy [36].

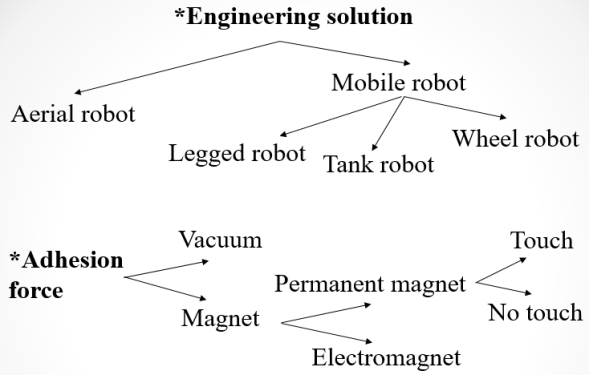

Fig. 1: Overall approach for steel bridge inspection robot.

In summary, the existing automated bridge inspection is described on a chart in Fig. 1. Robots, which fly, have electromagnets or utilize vacuum adhesion tend to have energy issues. These types of robots can not work for long periods of time out in the field, and tethering the devices using a wire for power is not feasible due to the oftentimes complicated and complex structures found on steel bridges. Climbing mobile robots work exceptionally well on simple and continuously contoured surfaces. However, steel bridge structures vary immensely; without standards of practice (Fig.2). There may be cylinders as Fig. 2(a, c) and or I beams, such as Fig. 2(b, d). It is difficult for conventional wheeled robots to work on these types of geometries commonly found on bridges. While legged robots can solve this issue with their mobile capabilities they struggle when moving on normal surfaces. The movement of worm or spider-like behavior becomes redundant and increasingly complicated in comparison to other wheeled designs. Each transportation method has its own difficulty getting around nuts (Fig. 2(b, d)) and still maintaining the adhesion force. Flying robots offer an effective approach without limitations of being adhered to the bridges surface. However, steel bridge maintenance requires a thorough inspection along the structural members of the bridge. Unfortunately, drones are not currently able to perform these in-depth analyses of structural steel members.

This paper presents a practical climbing robotic system, which combines the methods and subsequently the advantages of some of the other steel inspection robots created previously. The robot can adapt to a wide range of different sorts of bridge surfaces (flat, curving, rough). The hybrid approach implemented in the robot in this paper allows it to have both a mobile mode and a transforming mode (Fig. 4). These allow it to adapt to most complex steel bridge surfaces for efficient inspections. This robot utilizes adhesion force generated by permanent magnets in two modes; untouched magnets during mobile mode and touched for transforming mode. The flexible magnet array allows the robot to overcome obstacles including nuts and bolts. To demonstrate the robot's working principle, it has been deployed for climbing on indoor and outdoor steel structures and steel bridges.

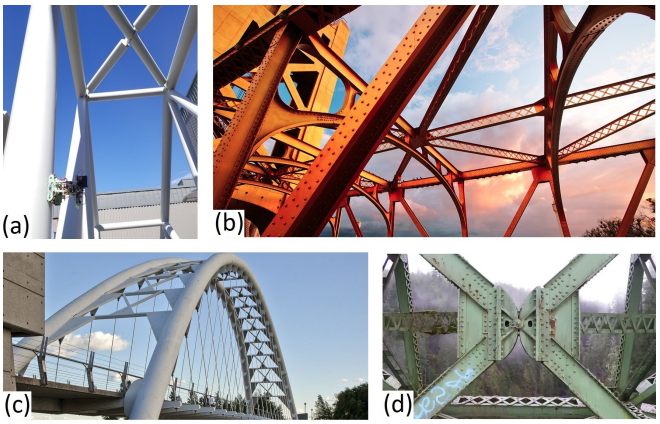

Fig. 2: (a) Cylinder steel bridge; (b) Complex I bar steel bridge with nuts; (c) A bridge with curving and plat surfaces; (d) A complicated joint.

II. Overall Design

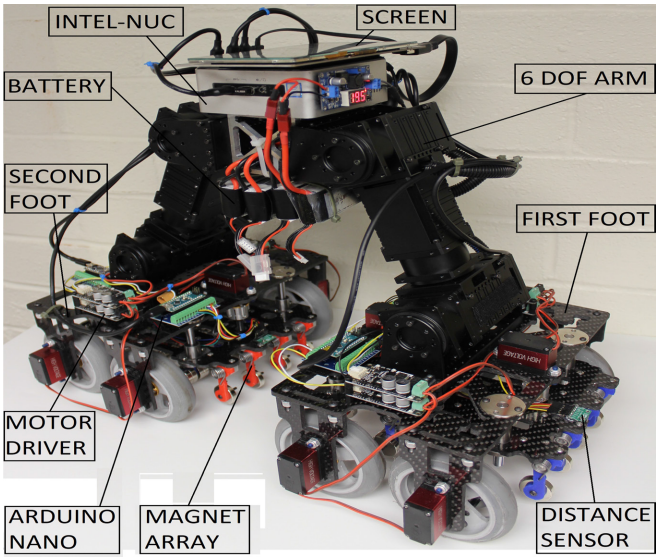

Fig. 3: Overall design of robot.

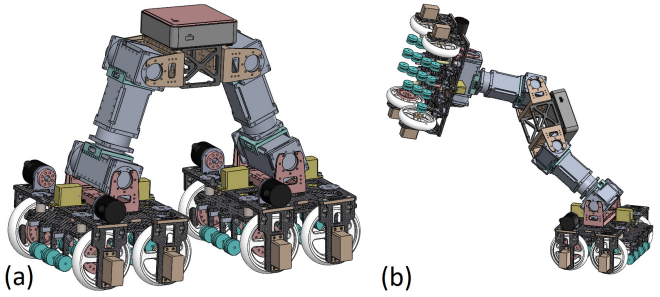

Fig. 4: Robot function (a) Mobile mode; (b) Transforming mode, or worm mode.

The design concept of the hybrid climbing robot is illustrated in Fig. 3 and it's function is described in Fig.4. The robot is divided into two main parts: the feet and body.

Each foot is loaded with permanent magnets for adhesion force therefore allowing the robot to expend no energy for its continued attachment to steel surfaces. In mobile mode the magnets hover in an untouched position with a 1mm distance from the steel surface. The magnets are ring shaped and arranged in an array, which allows the robot to pass nuts and bolts smoothly while still maintaining a full adhesion force. The torsion spring is instrumental in the design of the feet, they allow every single magnet cell to individually adapt to varying external stimuli and then return to its initial structure. The magnets utilized in the array are magnetized through their diameter as opposed to through their thickness as shown in Fig. 5. This allows them to be more suitable with their design purpose.

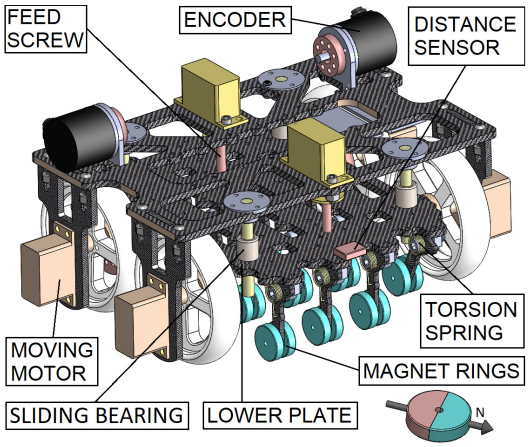

Fig. 5: The robots foot with flexible magnet array.

The distance between the magnet arrays and surface is controllable, and each foot is able to work in touched or untouched orientations. Two parallel feed screws are utilized with an actuator to enable the control system to modify the distance that each foot is kept at. Feedback from a distance sensor helps to ensure that the magnet arrays are kept at an optimal distance. The four wheels on each foot keep the robot stable when standing on one foot and support large moments while simultaneously being light weight. The rubber wheels maximize the friction factor between the robot and the surfaces that each foot is adhered to. The foot design allows the ARA robot to function on different surface conditions as described on Fig.6. The body has 6 degrees of freedom (DOF) and functions like a robot arm shown in Fig.7 when the robot is in transforming mode.

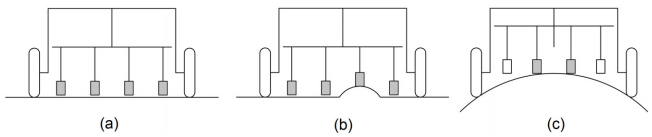

Fig. 6: (a) The robot on flat surface; (b) The robot passing nuts; (c) The robot on a curving surface.

When the robot encounters an area it is having difficulties traversing while in mobile mode, the robot will alter the magnet orientation of one foot to touched so that the robot

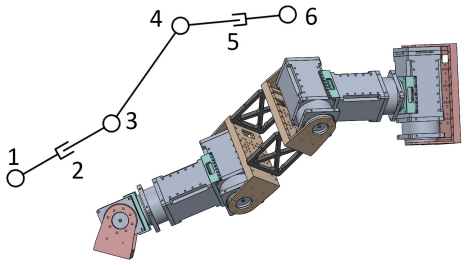

Fig. 7: The robot body - 6 DOF robot arm.

may shift into transforming mode to find a new surface to travel along and complete it's task. In transforming mode one foots magnet array will touch fully to the surface to maximize its adhesion force. Then the magnets on the second foot will move up to release the adhesion force. Now, the robot works as a 6 DOF robot arm. When touching a new surface, the process happens again to the opposite feet. This enables the robot to move the whole robot to new place. The whole process is shown in Fig. 8.

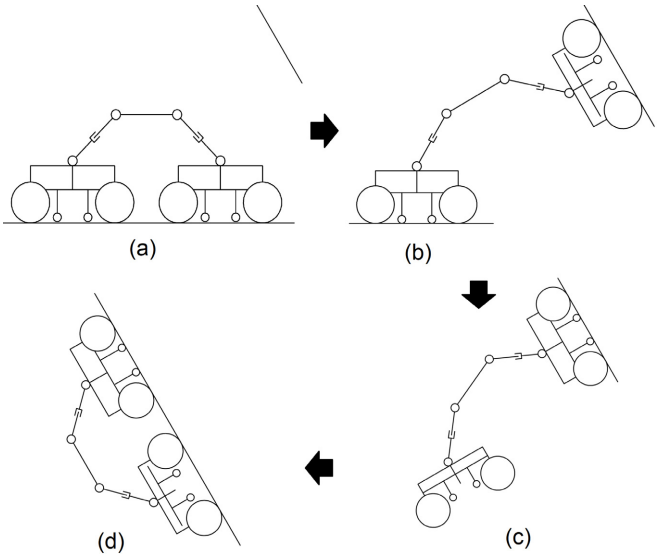

Fig. 8: Transformation process: (a) The robot in mobile mode; (b) The robot makes the magnet array touch on the 1st foot and looks for new a new surface with the other; (c) The 2nd foot touches a new surface and moves the rest of the robot there; (d) The robot switches back to mobile mode on the new surface.

III. Mechanical Design and Analysis

Throughout the design process of this robot, the ARA team performed an extensive set of statics analyses on the robot. These examinations into the mechanical behaviors behind which this robot has been constructed under, have allowed the ARA team to design and manufacture a robot, which surpasses the current capacities of other steel bridge inspection robots that came before it such as CROC [18], the inchworm inspired robot or MINOAS [25].

A. Transformation Analysis

The purpose of the transformation analysis was to determine the maximum moment the robot would experience under static conditions. This evaluation allowed us to determine

the moment the robot experiences when transforming and the minimum torque required from our servos to overcome the force of gravity.

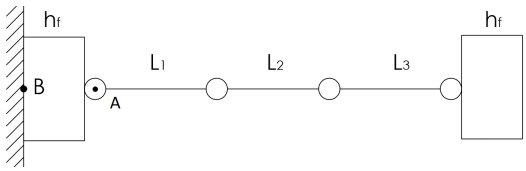

Fig. 9: Extended statics diagram.

Variable h_f represents the height of the feet, and m_f is the mass of foot. L_1, L_2, L_3 are the lengths of links, one through three. m_e is the mass of equipment that the robot is carrying. m_{L1}, m_{L2}, m_{L3} are the masses of their respective links. g is for gravity.

First, the moment acting at point A in Fig. 9 was determined in order to obtain a generic equation Equ. (1) to model the torque output required from a servo at point A as a function of the variables above. After this, the ARA team could decide upon a particular servo to use in the construction of the proposed robot.

$$\begin{aligned} T_A = &(\frac{1}{2}L_1)m_{L1}g + (L_1 + \frac{1}{2}L_2)(m_1 + m_e)g \\ &+ (L_1 + L_2 + \frac{1}{2}L_3)m_{L3}g \\ &+ (L_1 + L_2 + L_3 + \frac{1}{2}h_f)m_f g. \end{aligned} \tag{1}$$

The moment the robot experiences when fully extended was determined in this analysi,s which informed the team about how large the moment acting upon the robot would be through Equ. (2). In the Turn Over and Sliding Friction Analysis section later in this paper, we take the results of this study and use them as an input for the external moment that the foot is experiencing in the Turn Over Analysis.

$$\begin{aligned} M_B = &(\frac{1}{2}h_f)m_f g + (h_f + \frac{1}{2}L_1)m_{L1}g \\ &+ (h_f + L_1 + \frac{1}{2}L_2)(m_{L2} - m_e)g \\ &+ (h_f + L_1 + L_2 + \frac{1}{2}L_3)m_{L3}g \\ &+ (\frac{3}{2}h_f + L_1 + L_2 + L_3)m_f g. \end{aligned} \tag{2}$$

In both the Moment and Torque equations (1) and (2), the mass of the feet play a very large role in how large the respective acting moment and torque is. When we performed this analysis using aluminum as the material for the structural members of the robot, we found that our robot needed a very significant amount of torque to overcome gravity. From this, we concluded that our servos would have very low factors of safety. One of the ways in which the ARA team addressed this issue was by changing the material with which the structural members of the robot were manufactured from, choosing carbon fiber instead of aluminum.

The reduction of total mass in the feet gives our robot a much larger factor of safety to subsequently operate in a much more desirable manner. This reduction in mass (-40%) enables our robot to traverse steel structures because its servos can hoist the robot and hold still or over power the force of the moments acting on them. This means that the ARA robot is able to carry more equipment than it would have been able to if it was manufactured from aluminum.

B. Lower Plate Statics Analysis

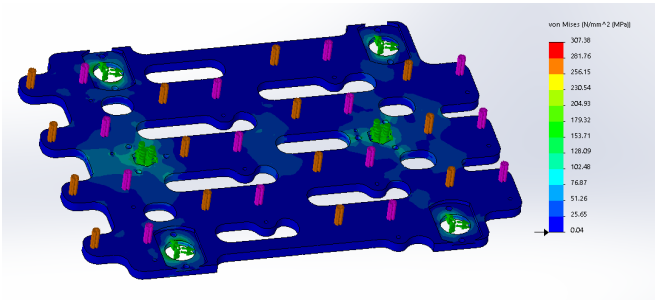

Fig. 10: Lower plate Solidworks static study simulation.

After the team decided to move forward with the use of carbon fiber, we needed to calculate the thickness of the material we would need for use on our robot. To do this, the ARA team employed the use of a 3D CAD software called Solidworks. The lower plate (Fig. 10) was chosen for analysis because the team determined that it would receive the most forces and therefore the most stress of all the other structural members in the design. Once a 3D model had been created, a statics study was made, then the team created all of the fixture conditions and forces, which would be acting on the plate. After this, the team created a custom material entry for the model using all of the material property characteristics of carbon fiber. For the purpose of this study, we assumed that our robot would be constructed from standard carbon fiber. We obtained these values from MatWeb, a material property database [37].

Solidworks statics studies approximate the stress that will be on various subsections of the frame by splitting up the 3D solid model into meshed chunks. Then, it takes into account the external forces and fixture conditions acting on the model and calculates the Von Mises stress [38] at each subsection of the mesh along the entire member Equ. (3). The generic equation for Von Mises stress, σ_v, is as follows:

$$\begin{aligned} \sigma_v = &[\frac{1}{2}[(\sigma_{11} - \sigma_{22})^2 + (\sigma_{22} - \sigma_{33})^2 \\ &+ (\sigma_{33} - \sigma_{11})^2 + 6(\sigma_{12}^2 + \sigma_{23}^2 + \sigma_{31}^2)]]^{\frac{1}{2}}. \end{aligned} \tag{3}$$

By iteratively running this simulation, the ARA team was able to examine a range of different thicknesses of carbon fiber. The team determined that while $4mms$ of thickness would meet the design requirements for the project, it also would have had a very low factor of safety of only 1.17. As a result, the team opted for a sturdier plate to ensure the structural members of the robot were not at risk of breaking

during use based on the calculated forces and moments from the transformation and turn over analyses.

C. Turn Over and Sliding Friction Analysis

At this point in the design process, the ARA team needed to conclude whether our robot would be at risk of toppling over or slipping while in use. To do this, we performed two more statics analyses, one, on an adhered foot with an external moment acting on it and the other as stationary foot adhered to a steel surface resisting sliding.

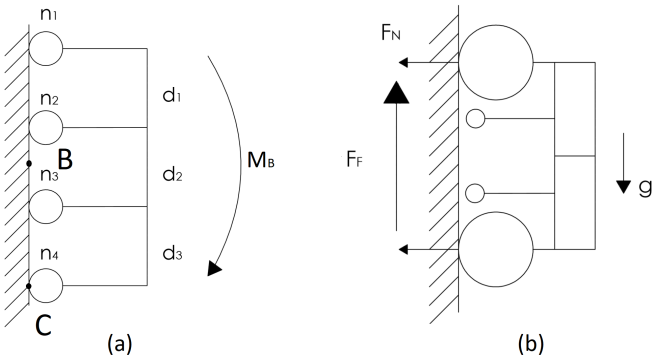

Fig. 11: Turn over/adhesion diagram.

Our turn over analysis (Fig. 11a) builds off of the transformation analysis by using the proposed moment function Equ. (2) as an input to the external moment acting upon the foot in this analysis. In order to determine how much adhesion force was required by each foot, a moment was taken at point C, this produced equations (4) and (5).

Variables n_1, n_2, n_3, n_4 represent the number of magnets in each row. M_C is the moment at point C, and F_{mag} is the force created by each magnet. d_1, d_2, d_3 all represent distances, where $M_B = f(h_f, m_f, m_{L1}, m_e, m_{L2}, m_{L3}, L_1, L_2, L_3, g)$, is solved for in the Transformation Analysis subsection of this paper.

$$\begin{aligned} M_c = & -M_B + F_{mag}n_3d_3 + F_{mag}n_2(d_2 + d_3) \\ & + F_{mag}n_1(d_1 + d_2 + d_3). \end{aligned} \tag{4}$$

Equ. (4) was then simplified and adjusted to emphasize the role magnet strength and each distance would have upon the net moment, M_C, giving Equ. (5).

$$\begin{aligned} M_c = & F_{mag}(d_3(n_1 + n_2 + n_3) + d_2(n_1 + n_2) \\ & + d_1n_1) - M_B = -M_B + F_{mag}n_3d_3 \\ & + F_{mag}n_2(d_2 + d_3) + F_{mag}n_1(d_1 + d_2 + d_3). \end{aligned} \tag{5}$$

The resulting equation Equ. (5) helped develop a better understanding about the importance of foot orientation, location of magnets, and the power of the magnets in the design. This analysis was also instrumental to the design layout of each of the feet in our robot and helped to ensure that the robot would maintain its position on steel structures.

The sliding friction analysis (Fig. 11b) assumes static conditions to determine what the required force of friction acting on the wheels is to prevent sliding. The main purpose of these calculations was to ensure that the robot's feet would not slide down the steel surfaces that they are adhered to.

i represents the number of wheels that the normal force (F_N) is distributed between, and n is for the total number of permanent magnets on the foot. F_F is the friction force, and F_{mag} is the force generated by one magnet. μ represents the friction coefficient between steel and rubber. For the purposes of our study, we used a value of 0.7 [39].

This evaluation begins by defining the equation for the normal force acting perpendicular to the surface that the robot is adhered to; Equ. (6).

$$F_N = \frac{nF_{mag}}{i}. \tag{6}$$

Then, a base equation is written to solve for the force of friction acting against motion, Equ. (7).

$$F_F = iF_N\mu. \tag{7}$$

Which when both combined, yields Equ. (8).

$$F_F = nF_{mag}\mu. \tag{8}$$

Equ.(8) models the force of friction as a function of the total number of magnets on the foot, the friction coefficient based on the materials in contact and the force generated by one magnet.

D. Lead Screw Analysis

Once the team had finalized the overall design of the robot and determined the strength of permanent magnets we would need, the ARA team then needed to calculate how much torque the servos on the feet would need to output in order to turn the lead screws attached to the lower plate of the foot. This capability allows the robots to modify the strength of their adhesion force to the steel surfaces they are on by raising and lowering the magnet arrays. In order to calculate

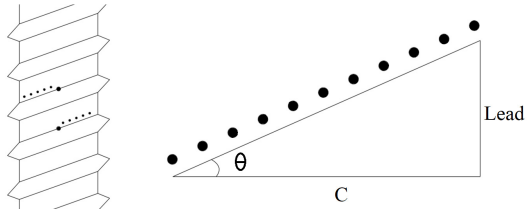

Fig. 12: Lead screw 'unrolling' diagram.

how much torque would be required, the ARA team needed to determine how much of the total adhering force from the magnets would translate into a moment in the lead screws, Equ. (9). The equation effectively 'unrolls' the thread (Fig. 12) to determine the angle at which a downward force would translate into creating a moment in the lead screws direction. The variable (θ) represents the pitch of the threading on the lead screws, and k is the numbers of servos on one foot. r_L is the radius of the lead screw, and m_{LA} is the mass of the lead screw. n is the number of permanent magnets on the lower frame, and F_{mag} is the force one magnet creates. C is the circumference of the lead screw.

$$\theta = tan^{-1}(\frac{lead * 1rev}{2\pi r_L}). \tag{9}$$

Next, the team needed to determine how much force would be acting upon the lower frame assembly of the robot. This was done by summing the combined forces of all the permanent magnets and the forces created due to gravity on the lower frame; yielding Equ. (10).

$$F_{LA} = \frac{nF_{mag}}{k} + m_{LA}g. \tag{10}$$

After this, the ARA team could then compute the moment the lead screws would experience as a function of their diameter, F_{LA}, and θ. This allowed our team to determine what servos we would need to overcome the required minimum torque described by Equ. (11).

$$T_L = r_L F_{LA} tan\theta. \tag{11}$$

IV. Robot Deployment

The purpose of the indoor testing was to evaluate the robots climbing abilities (Fig. 13) and examine how adhesion force varied with distance from the steel surface.

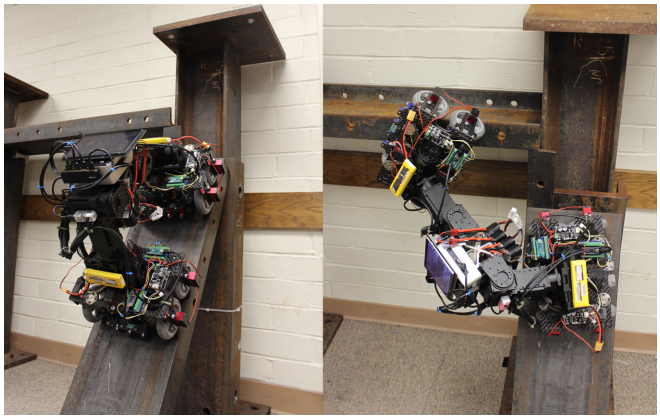

Fig. 13: The robot being tested on a steel structure indoors.

The ARA Labs robot was able to successfully climb the lab's steel beams (Fig. 13). With the ARA robot's climbing capabilities verified, the robot was then tested outside on more complex structures than what could be found in the lab.

Outdoor testing for the robot began at a local steel art statue on the university campus famous for having every commercial steel link type on it, as showcased in Fig 14.

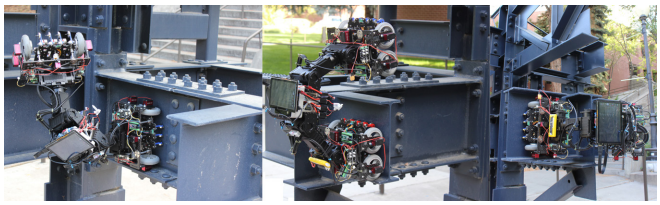

Fig. 14: Deployment of the robot on a steel structure.

At this art statue, the team was able to examine the robot's physical ability to traverse the complex geometries, which would come across out in the world as show in Fig. 14. The results from this assessment and verification subsection showcase the ARA Lab robot's proposed ability to get around and traverse complex, jagged geometries like those found on the art statue, Fig. 14. The testing at this art statue suggests that more work should be put into creating friction to resist twisting while the robot is in worming mode. While not entirely crippling, the robot did struggle to maintain its orientation when moving. This issue was also likely exacerbated by a rudimentary controller design, which creates sharp, sudden movements that ended as quickly as they began. Smoothing of the accelerations created by the servos will be imperative in ensuring this robot is capable of meeting commercial demands for steel structure inspection.

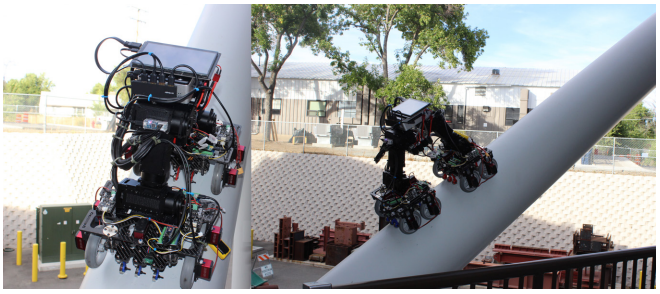

Fig. 15: Mobile mode example on bridge.

Additional evaluations were done at a bridge on campus, which is comprised of long cylindrical members. As shown in Fig. 15, these members were useful for testing the robots ability to adhere to round surfaces.

Link to the video demonstration of the robot deployments can be seen here: `https://youtu.be/PwDf6h0Om3c`

V. Conclusion and Future Work

The ARA team's robot described by this paper proposes a design, which combines the best parts of other modern day steel inspection robots in order to traverse the complex geometries commonly found on steel structures such as windmills, steel bridges and buildings. The largest challenge so far in this project has been making sure that the robot will function as intended. Since the team is implementing a design, which draws from a wide range of other designs, the robot needs to be able to accommodate all of the design parameters for each design in order to maintain the intended functionalities of the implemented features. This created a necessity for detailed design analyses to ensure that such an amalgamation of various designs could successfully work together in unison.

In the future, the ARA team plans to design a working arm for the ARA Lab robot so that it may carry special equipment such as an eddy current sensor to assist with performing detailed inspections of dangerous, hard to reach places on steel structures. The team would also like to address the robots ability to resist twisting by increasing the amount of friction the robot generates with a steel surface during the robots articulations in transforming mode. Additionally, autonomous localization, navigation and sensing function will be developed to allow the robot to perform automated inspection. Our previous work on this localization, navigation and sensing for bridge deck inspection robots [40]–[45] will be utilized for this future development.

REFERENCES

[1] U.S Department of transportation highway administration, national bridge inventory data, 2019. http://www.fhwa.dot.gov/bridge/nbi.cfm.

[2] Washington bridge collapse, 2013. https://www.cnn.com/2013/05/24/us/gallery/skagit-river-bridge/index.html.

[3] A. McCrea, D. Chamberlain, and R. Navon. Automated inspection and restoration of steel bridges – a critical review of methods and enabling technologies. *Automation in Construction*, 11(4):351 – 373, 2002.

[4] B. Purna Chandra Rao. *Non-destructive Testing and Damage Detection*, pages 209–228. Springer Singapore, Singapore, 2017.

[5] Crews inspect condition of golden gate bridge's towers, April 30, 2018. https://www.nbcbayarea.com/on-air/as-seen-on/Crews-Inspect-Condition-of-Golden-Gate-Bridge_s-Towers_Bay-Area-481315951.html.

[6] W. Shen, J. Gu, and Y. Shen. Permanent magnetic system design for the wall-climbing robot. In *IEEE Intern. Conf. Mechatronics and Automation, 2005*, volume 4, pages 2078–2083 Vol. 4, July 2005.

[7] S. T. Nguyen and H. M. La. Development of a steel bridge climbing robot. In *Intelligent Robots and Systems, 2019. IROS 2019. IEEE/RSJ Intern. Conf. on*, Nov 2019.

[8] Anh Q. Pham, Hung M. La, Kien T. La, and Minh T. Nguyen. A magnetic wheeled robot for steel bridge inspection. In Kai-Uwe Sattler, Duy Cuong Nguyen, Ngoc Pi Vu, Banh Tien Long, and Horst Puta, editors, *Advances in Engineering Research and Application*, pages 11–17, Cham, 2020. Springer International Publishing.

[9] R. Wang and Y. Kawamura. A magnetic climbing robot for steel bridge inspection. In *Intelligent Control and Automation (WCICA), 2014 11th World Congress on*, pages 3303–3308, June 2014.

[10] H. M. La, T. H. Dinh, N. H. Pham, Q. P. Ha, and A. Q. Pham. Automated robotic monitoring and inspection of steel structures and bridges. *Robotica*, 37(5):947 – 967, May 2019.

[11] S. T. Nguyen and H. M. La. Roller chain-like robot for steel bridge inspection. In *the 9th International Conference on Structural Health Monitoring of Intelligent Infrastructure (SHMII-9)*, Aug 2019.

[12] D. Zhu, J. Guo, C. Cho, Y. Wang, and K. Lee. Wireless mobile sensor network for the system identification of a space frame bridge. *IEEE/ASME Trans. on Mechatronics*, 17(3):499–507, June 2012.

[13] G. Lee, G. Wu, J. Kim, and T. Seo. High-payload climbing and transitioning by compliant locomotion with magnetic adhesion. *Robotics and Autonomous Systems*, 60(10):1308 – 1316, 2012.

[14] T. Seo and M. Sitti. Tank-like module-based climbing robot using passive compliant joints. *IEEE/ASME Transactions on Mechatronics*, 18(1):397–408, Feb 2013.

[15] R. Wang and Y. Kawamura. A magnetic climbing robot for steel bridge inspection. In *Proceeding of the 11th World Congress on Intelligent Control and Automation*, pages 3303–3308, June 2014.

[16] J. Guo, W. Liu, and K. M. Lee. Design of flexonic mobile node using 3d compliant beam for smooth manipulation and structural obstacle avoidance. In *2014 IEEE Intern. Conf. on Robotics and Automation (ICRA)*, pages 5127–5132, May 2014.

[17] S. Kamdar. Design and manufacturing of a mecanum sheel for the magnetic climbing robot. *Master Thesis, Embry-Riddle Aeronautical University*, May 2015.

[18] P. Ward, P. Manamperi, P. R. Brooks, P. Mann, W. Kaluarachchi, L. Matkovic, G. Paul, C. H. Yang, P. Quin, D. Pagano, D. Liu, K. Waldron, and G. Dissanayake. Climbing robot for steel bridge inspection: Design challenges. In *Austroads Publications Online, ARRB Group*, 2015.

[19] N. H. Pham and H. M. La. Design and implementation of an autonomous robot for steel bridge inspection. In *54th Allerton Conf. on Comm., Con., and Comp.*, pages 556–562, Sept 2016.

[20] R. Wang and Y. Kawamura. Development of climbing robot for steel bridge inspection. *Industrial Robot: An International Journal*, 43(4):429–447, 2016.

[21] N. H. Pham, H. M. La, Q. P. Ha, S. N. Dang, A. H. Vo, and Q. H. Dinh. Visual and 3d mapping for steel bridge inspection using a climbing robot. In *The 33rd Intern. Symposium on Automation and Robotics in Construction and Mining (ISARC)*, pages 1–8, July 2016.

[22] Y. Takada, S. Ito, and N. Imajo. Development of a bridge inspection robot capable of traveling on splicing parts. *Inventions*, 2, 2017.

[23] F. Tche, W. Fischer, G. Caprari, R. Siegwart, R. Moser, and F. Mondada. Magnebike: A magnetic wheeled robot with high mobility for inspecting complex-shaped structures. *Journal of Field Robotics*, 26(5):453–476, 2009.

[24] M. Tavakoli, C. Viegas, L. Marques, J. N. Pires, and A. T. de Almeida. Omniclimbers: Omni-directional magnetic wheeled climbing robots for inspection of ferromagnetic structures. *Robotics and Autonomous Systems*, 61(9):997 – 1007, 2013.

[25] M. Eich and T. Vgele. Design and control of a lightweight magnetic climbing robot for vessel inspection. In *the 19th Mediterranean Conf. on Control Automation*, pages 1200–1205, June 2011.

[26] A. Leibbrandt, G. Caprari, U. Angst, R. Y. Siegwart, R.J. Flatt, and B. Elsener. Climbing robot for corrosion monitoring of reinforced concrete structures. In *Applied Robotics for the Power Industry (CARPI), the 2nd Intern. Conf. on*, pages 10–15, Sept 2012.

[27] H. Leon-Rodriguez, S. Hussain, and T. Sattar. A compact wall-climbing and surface adaptation robot for non-destructive testing. In *Control, Automation and Systems (ICCAS), 2012 12th Intern. Conf. on*, pages 404–409, Oct 2012.

[28] A. San-Millan. Design of a teleoperated wall climbing robot for oil tank inspection. In *Control and Automation (MED), 2015 23th Mediterranean Conference on*, pages 255–261, June 2015.

[29] W. Shen, J. Gu, and Y. Shen. Proposed wall climbing robot with permanent magnetic tracks for inspecting oil tanks. In *IEEE Intern. Conf. Mechatronics and Automation, 2005*, volume 4, pages 2072–2077 Vol. 4, July 2005.

[30] Versatrax 100^{TM}. http://inuktun.com/en/products/.

[31] Bridgebot. http://www.robotics.umd.edu/content/maryland-robotics-center-videos/.

[32] T. Bandyopadhyay, R. Steindl, F. Talbot, N. Kottege, R. Dungavell, B. Wood, J. Barker, K. Hoehn, and A. Elfes. Magneto: A versatile multi-limbed inspection robot. In *2018 IEEE/RSJ Inter. Conf. on Intelligent Robots and Systems (IROS)*, pages 2253–2260, Oct 2018.

[33] A. Mazumdar and H. H. Asada. Mag-foot: A steel bridge inspection robot. In *Intelligent Robots and Systems, 2009. IROS 2009. IEEE/RSJ Intern. Conf. on*, pages 1691–1696, Oct 2009.

[34] Elios2. https://www.youtube.com/watch?v=hW1Fn32JBls/.

[35] Case study: Advancing bridge inspections with intel's drone solutions, accessed on September 15, 2019. https://www.intel.com/content/www/us/en/products/docs/drones/advancing-bridge-inspections-case-study.html.

[36] Birds. https://inspire-utc.mst.edu/researchprojects/as-4/.

[37] Carbon fiber material properties. http://www.matweb.com/search/datasheettext.aspx?matguid=39e40851fc164b6c9bda29d798bf3726.

[38] Summary of von mises yield criterion. http://web.mit.edu/nnf/education/Summer2009/Von_Mises_Yield$%$20Criterion.pdf.

[39] Coefficients of friction for steel. https://hypertextbook.com/facts/2005/steel.shtml.

[40] H. M. La, R. S. Lim, B. B. Basily, N. Gucunski, J. Yi, A. Maher, F. A. Romero, and H. Parvardeh. Mechatronic systems design for an autonomous robotic system for high-efficiency bridge deck inspection and evaluation. *IEEE/ASME Transactions on Mechatronics*, 18(6):1655–1664, Dec 2013.

[41] H. M. La, N. Gucunski, Seong-Hoon Kee, J. Yi, T. Senlet, and Luan Nguyen. Autonomous robotic system for bridge deck data collection and analysis. In *2014 IEEE/RSJ Intern. Conf. on Intelligent Robots and Systems*, pages 1950–1955, Sep. 2014.

[42] H. M. La, N. Gucunski, K. Dana, and S.-H. Kee. Development of an autonomous bridge deck inspection robotic system. *Journal of Field Robotics*, 34(8):1489–1504, 2017.

[43] S. Gibb, H. M. La, T. Le, L. Nguyen, R. Schmid, and H. Pham. Nondestructive evaluation sensor fusion with autonomous robotic system for civil infrastructure inspection. *Journal of Field Robotics*, 35(60), 2018.

[44] H. M. La, N. Gucunski, S.H. Kee, and L.V. Nguyen. Visual and acoustic data analysis for the bridge deck inspection robotic system. In *The 31st International Symposium on Automation and Robotics in Construction and Mining (ISARC)*, pages 50–57, July 2014.

[45] H. M. La, N. Gucunski, S.-H. Kee, and L.V. Nguyen. Data analysis and visualization for the bridge deck inspection and evaluation robotic system. *Visualization in Engineering*, 3(1):1–16, 2015.